

Synthesis and Characterization of Some Long-Chain Diesters with Branched or Bulky Moieties

Gerhard Knothe*, Robert O. Dunn, Michael W. Shockley¹, and Marvin O. Bagby²

ARS, USDA, NCAUR, Peoria, Illinois 61604

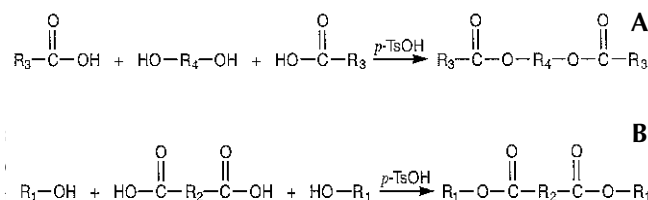
ABSTRACT: Several novel fatty diesters with bulky moieties were synthesized by esterification of mono- or bifunctional fatty acids or with mono- or bifunctional alcohols using *p*-toluenesulfonic acid as catalyst. They were characterized by ¹H and ¹³C nuclear magnetic resonance as well as positive chemical ionization (PCI) mass spectrometry. The PCI mass spectra of the resulting diol diesters and diacid diesters are discussed and compared. The compounds were investigated as potential additives for improving the cold flow properties of vegetable oil esters used as biodiesel.

Paper no. J9343 in *JAOCs* 77, 865–871 (August 2000).

KEY WORDS: Additives, biodiesel, diacid diesters, diol diesters, low-temperature flow properties, mass spectrometry, nuclear magnetic resonance.

Long-chain compounds with branched or bulky moieties find uses in various commercial products. In biodiesel (1,2), an alternative diesel fuel derived from vegetable oils or animal fats, branched esters such as neat isopropyl or isobutyl esters have been applied to improve the low-temperature properties as documented by cloud and pour points (3–5). The use of branched esters constitutes one of the possible solutions for improving the low-temperature properties of biodiesel, the others being dilution with conventional diesel fuel, the use of various polymeric additives (1,2), and winterization (6–9). Other compounds with branched or bulky moieties, such as neopentylglycol diesters, are used commercially in lubricants (10–15), plasticizers (16,17), cosmetics (18), and even edible fat replacers (19,20).

The present long-chain compounds were synthesized by *p*-toluenesulfonic acid (*p*-TsOH)-catalyzed esterification of acids and alcohols in toluene. Either diols were reacted with acids or diacids were reacted with alcohols (see Scheme 1A and 1B, respectively). One of the reactants was monofunctional whereas the other was bifunctional. 2-Octanol was cho-



SCHEME 1

glutaric acid). Scheme 1 and Table 1 provide information on the exact nature of the compounds studied here. The compounds arising from the reaction of monoacids with diols will be termed diol diesters and those derived from diacids with monohydric alcohols will be termed diacid diesters in the following text. Besides studying the potential application of these compounds as additives in vegetable oil-based alternative diesel fuels, their analytical characterization, especially by positive chemical ionization (PCI) mass spectrometry (MS) and ¹³C nuclear magnetic resonance (NMR), is reported.

Some other patent syntheses (21,22) of compounds such as the present ones have been reported. Nonpatent syntheses include some compounds with neopentylglycol as diol (23), compounds derived from α,α -dimethylalkanoic acids and polyols (24), esters from dodecanedioic acid, and mono-alcohols (25) as well as the enzymatic synthesis of related wax esters (26). Besides their synthesis, the mass spectrometric

TABLE 1
Some Compounds Synthesized in the Present Work

Diol diesters		
Entry	Acid	Diol
a	Lauric	1,4-Di(hydroxymethyl)cyclohexane
b	Hexanoic	Neopentylglycol
c	Hexanoic	1,4-Di(hydroxymethyl)cyclohexane
d	3,6-Dioxaheptanoic	1,4-Di(hydroxymethyl)cyclohexane
Diacid diesters		
Entry	Diacid	Alcohol
e	3,3-Dimethylglutaric	2-Octanol
f	Suberic	2-Octanol
g	1,4-Cyclohexanedicarboxylic	2-Octanol

*To whom correspondence should be addressed at USDA, ARS, NCAUR, 1815 N. University St., Peoria, IL 61604.
E-mail: knothegh@mail.ncaur.usda.gov

¹Present address: Caterpillar, Inc., Tech Center—E, P.O. Box 1875, Peoria, IL 61656-1875.

²Retired.

behavior of compounds similar to the present ones was studied, including esters of neopentyl glycol (27), other esters of polyols of neopentane (28–33), the decomposition products of neopentylglycol dilaurate (34), and ethane (35,36) and propanediol (35) diesters.

EXPERIMENTAL PROCEDURES

All starting materials were purchased from Aldrich (Milwaukee, WI) except 3,6-dioxaheptanoic acid (“oxa” indicating replacement of CH_2 by O in the chain), which was obtained from Hoechst (Frankfurt am Main, Germany). Solvents were supplied by Fisher Scientific (Fair Lawn, NJ) or Aldrich. Methyl soyate (biodiesel) was obtained from Ag Environmental Products (Lenexa, KS).

High-performance liquid chromatography (HPLC) equipment consisted of a preparative-scale pump (obtained from MidAmerica Analytical Instruments, St. Louis, MO), a Rainin (Varian Chromatography Systems, Walnut Creek, CA) Dynamax 60 Å silica column (41.4 mm i.d.), a Kratos (PerkinElmer Corp., Norwalk, CT) Spectroflow 757 ultraviolet (UV) absorbance detector, and a Waters (Millipore Corp., Milford, MA) R401 differential refractometer detector. The runs were monitored on a chart recorder and a personal computer equipped with Justice (Mountain View, CA) HPLC software.

Mass spectra were obtained on a gas chromatography (GC)–MS system consisting of a Hewlett-Packard (Palo Alto, CA) 5890 Series II Plus gas chromatograph equipped with a DB-5MS capillary column (30 m \times 0.25 mm i.d.) attached to a Hewlett-Packard 5989B mass spectrometer operating in electron ionization (70 eV) or PCI mode (methane as reagent gas, 230 eV) using methane as reagent gas. All PCI spectra were background-subtracted. NMR spectra were obtained on a Bruker (Rheinstetten, Germany) ARX-400 spectrometer operating at 400 MHz (^1H NMR) or 100 MHz (^{13}C NMR). The solvent was CDCl_3 .

General synthetic procedure. All syntheses were carried out by mixing the starting materials (10 g acid component; 60 mol% diol relative to the acid when synthesizing diol diesters, 220 mol% alcohol relative to the acid when synthesizing diacid diesters) in toluene with 10 mol% *p*-TsOH relative to the acid component as catalyst. The reaction apparatus consisted of a flask equipped with a Dean-Stark trap and reflux condenser. The reaction mixture was refluxed for 6 h. Workup consisted of adding 100 mL of saturated aqueous NaHCO_3 solution and then extracting with 5 \times 50 mL diethyl ether. The combined organic layers were washed with saturated KCl solution and then dried over MgSO_4 . They were then filtered, the solvent removed on a rotary evaporator, and the product placed under vacuum for 2 h at 60°C. Yields ranged from 70% to nearly quantitative (97%) for these reactions. Reaction products were finally purified by HPLC using hexane as solvent except for entry f in Table 1 for which 1:1 hexane/dioxane was used. The products were liquids at ambient temperature except entry a in Table 1 (m.p.

53.7–55.6°C).

Low-temperature studies. Cloud points (CP) and pour points (PP) were determined according to ASTM standard methods D97 (PP) and D2500 (CP) (both obtained from Koehler Instrument Co., Bohemia, NY).

RESULTS AND DISCUSSION

Various moieties were incorporated to give bulky substituents or branching in the products (for a listing of compounds synthesized here, see Table 1). These kinds of structures may render the products useful as additives for improving the low-temperature properties of vegetable oil methyl esters used as alternative diesel fuel (biodiesel). Note that compounds with cyclohexyl moieties were obtained as *cis/trans* isomers as shown by NMR and two peaks giving identical mass spectra in GC–MS. No attempt was made to separate the isomers. The products were characterized by ^1H NMR, ^{13}C NMR, and MS. Spectroscopic characterization of the compounds will be discussed first and then the low-temperature studies.

MS. Generally, electron impact (EI) spectra of the present compounds are somewhat more complex than those obtained by methane PCI. The enhanced complexity is especially noticeable in the region $m/z < 100$. This is due to fragments resulting from rearrangements, cyclizations, etc., occurring more prominently in the EI spectra. Essential features of EI–MS of diesters of neopentylglycol, 1,2-ethanediol, and the propanediols have been discussed (27,35,36). Methane PCI usually yields spectra in which the peaks at higher m/z , which are strongly related to straightforward features such as chain lengths of the original molecules, are more intense and the molecular ion is always present, removing any ambiguities about the molecular weight of the sample.

The compounds whose spectra are depicted in Figure 1 and discussed as examples contain a neopentylglycol moiety and the diacid congener 3,3-dimethylglutaric acid as well as di(hydroxymethyl)cyclohexane and cyclohexanedicarboxylic acid moieties (entries a, c, d, f, h, and j in Table 1). The EI spectra will not be discussed in detail because this has been largely accomplished in the literature (27,35,36). The four mass spectra depicted in Figure 1 serve to illustrate the methane PCI mass spectral features of the present compounds.

PCI with methane as reagent gas yielded significant distinctive peaks at higher masses for the present compounds. This coincides with the mass spectral studies on branched di-Guerbet esters (37), where PCI was found to give distinctive m/z peaks at higher abundances and at higher mass ranges. Cleavages yielding the distinctive fragments are shown in Figure 2.

Generally, the methane PCI mass spectra of the diacid diesters display more peaks than those of the diol diesters. The spectra of bis-(2-octyl)-3,3-dimethylglutarate (Fig. 1A) and bis-(2-octyl)-1,4-cyclohexane dicarboxylate (Fig. 1B) are very similar despite the differences in the nature of the diacid. The mass spectra of diol diesters (Figs. 1C and 1D), however, differ depending on the nature of the diol moiety. Note that

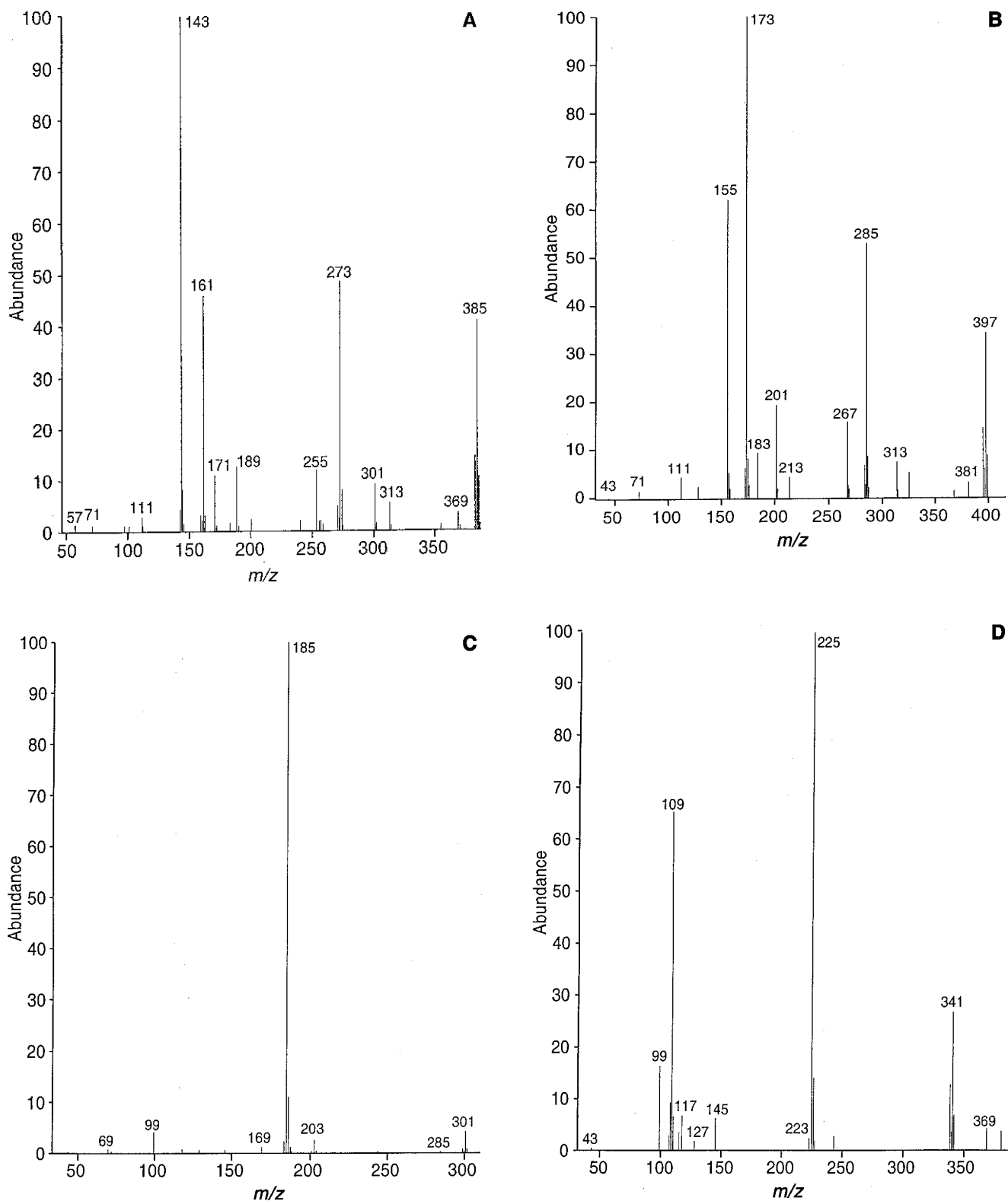


FIG. 1. Positive chemical ionization mass spectra of (A) bis-(2-octyl) 3,3-dimethyl glutarate, (B) bis-(2-octyl) 1,4-cyclohexanedicarboxylate, (C) neopentylglycol bis-hexanoate, and (D) 1,4-cyclohexanedimethanol bis-hexanoate.

the diol moiety in the diol diesters resembles that of the diacid moiety in the diacid diesters. Major cleavages for diacid diesters are depicted in Figure 2A and those for diol diesters in

Figure 2B.

Diacid diesters. The diacid diesters exhibit three major clusters of peaks. The first one is due to diacid diesters ex-

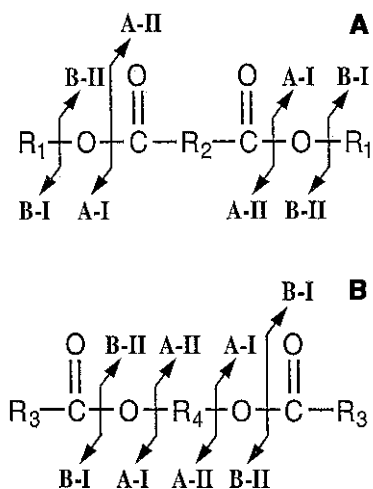


FIG. 2. Cleavages in methane positive chemical ionization mass spectrometry of (A) diacid diesters and (B) diol diesters.

hibiting strong $[M + H]^+$ and $[M - H]^+$ (which may correspond to $[M + H]^+ - H_2$, see Ref. 38) peaks. Straight-chain fatty acid methyl esters exhibit such behavior (38). Loss of hydrocarbon moieties at high m/z , for example $[M - 15]^+$, leads to peaks such as m/z 381 in Figure 1B and m/z 369 in Figure 1A.

A second cluster of peaks results from one cleavage fragment B-II in Figure 2A to give the monoester monoacid fragment that is protonated leading to m/z 273 in Figure 1A and m/z 285 in Figure 1B. Liberation of water causes the peaks at m/z 255 and m/z 267, respectively. Monoester monoacids are also detected as adducts with $C_2H_5^+$ (peaks at m/z 301 in Fig. 1A and m/z 313 in Fig. 1B). Such adduct formations are common in the mass spectra of straight-chain fatty acid methyl esters with methane as reagent gas due to its low proton affinity (38).

The third cluster of peaks in the methane PCI mass spectra of the diacid diesters results from both B-II cleavages in Figure 2A to give the protonated diacid (m/z 161 in Fig. 1A, m/z 173 in Fig. 1B). In both cases, the liberation of water gives the peaks at m/z 155 and m/z 143, respectively. Peaks related to the diacid are the base peak in both spectra (dehydrated diacid in Fig. 1A, protonated diacid in Fig. 1B). The diacid and its dehydrated derivative both form adducts with $C_2H_5^+$ to give the peaks at m/z 171 and 189 in Figure 1A and m/z 183 and 201 in Figure 1B. Note that m/z 171 in Figure 1A could be explained from a cleavage within the dimethylglutaric acid moiety but likely arises as discussed because the corresponding peak (at different m/z) is present in Figure 1B.

Diol diesters. A similar cleavage pattern holds for the diol diesters, although in these cases fewer peaks are observed (Figs. 1C and 1D) compared to the diacid diesters. $[M + H]^+$ and $[M - H]^+$ are found in both cases. These peaks are stronger in Figure 1D, and adduct formation is observed here also (m/z 369). The peak at m/z 225 in Figure 1D results from one cleavage A-II in Figure 2B. In Figure 1C, a peak at m/z 203 for the protonated monoester monoalcohol is observed

resulting from one cleavage B-II in Figure 2B. However, further liberation of water gives rise to the base peak at m/z 185. Direct cleavage A-II in the spectrum in Figure 1C contributing to m/z 185 cannot be excluded. Thus, successive loss of hexanoic acid ($m/z = 116$) would be responsible for the ion series 301 (protonated molecular ion) \rightarrow 185 \rightarrow 69. The differences in the spectra depicted in Figures 1C and 1D can likely be explained by greater stability of the cyclohexyl-containing moiety in the diester causing the spectrum in Figure 1D. The significantly greater stability of the cyclohexyl-containing fragment is additionally demonstrated by the presence of m/z 109 as strong/base peak in Figure 1D. This peak corresponds to the fragment depicted in Figure 2C. The loss of hexanoic acid is again shown in Figure 2D by the ion series m/z 341 \rightarrow 225 \rightarrow 109. The corresponding EI mass spectrum (not shown) exhibits m/z 108, which corresponds to further deprotonation of the m/z 109 fragment as the base peak. Both EI and PCI spectra exhibit m/z 99 (acylium ion from the monoacid), which corresponds to fragment B-I in Figure 2B. However, in Figure 1D, m/z 117 corresponding to protonated hexanoic acid (note adduct formation at m/z 145) is observed. The intensity of m/z 99 is greater in Figure 1D than in 1C, leading to the conclusion that liberation of water from m/z 117 contributes significantly here. In Figure 1C, m/z 117 is nearly completely absent.

The distinctive fragments in methane PCI-MS for selected compounds synthesized in the present work are listed in Table 2. No detailed further assignments are made in Table 2, because they correspond to the examples whose patterns are discussed.

NMR spectroscopy. Table 2 also contains data for the 1H and ^{13}C NMR spectra of compounds synthesized. The main features of the ^{13}C NMR spectra will be discussed here briefly.

In the diol diester derived from neopentyl glycol, the three ^{13}C NMR signals of the diol moiety occur at 68.91 (carbons attached to the oxygen), 34.54 (quaternary carbon), and 21.70 ppm (methyl carbons). In the diacid diester derived from 3,3-dimethylglutaric acid, the signal for the carbons attached to the ester moieties is at 45.68 ppm, that of the quaternary carbon is at 32.61 ppm, and that of the methyl groups is at 27.52 ppm. These assignments are confirmed through DEPT (distortionless enhancement of polarization transfer) NMR experiments, which distinguish carbons with odd and even numbers of protons as well as no attached protons.

The diesters with cyclohexyl moieties exist as *cis/trans* isomers (as the cyclohexyl-containing starting materials were already *cis/trans* isomers). In addition to these samples eluting during GC-MS investigations as two peaks, ^{13}C NMR is also useful for showing the existence of two isomers. The cyclohexyl moiety of corresponding diol diester has signals at 37.00–37.05 and 34.40–34.45 ppm (C_1 and C_4 tertiary carbons of the cyclohexyl moiety) and 28.80 and 25.25–25.30 ppm (C_2 , C_3 , C_5 , and C_6 secondary carbons of the cyclohexyl moiety). These assignments were confirmed again *via* DEPT experiments. The *cis* and *trans* isomers were not assigned

TABLE 2
Positive Chemical Ionization Mass Spectrometry (PCI-MS) Peaks (methane as reagent gas) and Nuclear Magnetic Resonance (NMR) Signals of Some of the Compounds Synthesized in the Present Work

Entry ^a	PCI-MS	¹ H NMR	¹³ C NMR
a	175 (100%), 157 (90%), 287 (55%), 399 (39%), 203 (20%), 185 (17%), 400 (11%), 269 (10%), 176 (9%), 397 (9%), 285 (8%)	3.97 (<i>d</i> , <i>J</i> = 7.2 Hz), 3.88 (<i>d</i> , <i>J</i> = 6.5 Hz), 2.28 (<i>t</i> , <i>J</i> = 7.5 Hz), 1.79 (<i>d</i>), 1.60 (<i>t</i>), 1.26 (<i>m</i>), 0.99 (<i>m</i>), 0.86 (<i>t</i>)	163.94, 69.10, 66.90 (5:1 ratio), 37.03, 34.44, 34.33, 31.86, 29.55, 29.43, 29.29, 29.22, 29.13, 28.81, 25.27, 25.00, 22.64, 14.07
b	301 ([<i>M</i> + 1] ⁺ , 4%), 203 (3%), 186 (11%), 185 (100%), 99 (4%)	3.84 (<i>s</i>), 2.27 (<i>t</i>), 1.58 (quintuplet), 1.29–1.24 (<i>m</i>), 0.92 (<i>s</i>), 0.85 (<i>t</i>)	173.66, 68.91, 34.54, 34.19, 31.24, 24.60, 22.24, 21.70, 13.83
c	369 (adduct, 4%), 341 ([<i>M</i> + 1] ⁺ , 65%), 339 ([<i>M</i> – 1] ⁺ , 18%), 225 (97%), 109 (100%), 99 (20%)	3.96 (<i>d</i>), 3.86 (<i>d</i>) (14:6 ratio), 2.26 (<i>t</i>), 1.79–1.24 (<i>m</i>), 0.97 (<i>m</i>), 0.86 (<i>t</i>)	173.89, 69.07, 66.88 (3:1 ratio), 37.02, 34.42, 34.26, 31.26, 28.79, 25.25, 24.64, 22.25, 13.84
d	377 ([<i>M</i> + 1] ⁺ , 32%), 244 (15%), 243 (100%), 163 (adduct, 11%), 135 (60%), 109 (41%), 89 (11%), 59 (5%)	4.04 (<i>s</i>), 3.97 (<i>d</i>), 3.87 (<i>d</i>), 3.61(<i>m</i>), 3.48 (<i>m</i>), 3.27 (<i>s</i>)	170.21, 71.61, 70.49, 69.22, 68.27, 67.06, 58.69, 36.64, 34.07, 28.40, 24.89
e	385 ([<i>M</i> + 1] ⁺ , 41%), 383 ([<i>M</i> – 1] ⁺ , 15%), 369 ([<i>M</i> – CH ₃] ⁺ , 4%), 313 (6%), 301 (adduct, 10%), 273 (49%), 255 (12%), 189 (adduct, 13%), 171 (11%), 161 (46%), 143 (100%)	4.84 (sextuplet), 2.33 (<i>t</i>), 1.52–1.20 (<i>m</i>), 1.15 (<i>d</i>), 1.06 (<i>s</i>), 0.82 (<i>t</i>)	171.42, 70.66, 45.68, 35.89, 32.61, 31.68, 29.05, 27.52 (CH ₃), 25.34, 22.50, 19.94, 13.98
f	399 ([<i>M</i> + 1] ⁺ , 28%), 397 ([<i>M</i> – 1] ⁺ , 10%), 383 ([<i>M</i> – CH ₃] ⁺ , 2%), 315 (adduct, 6%), 287 (60%), 285 (8%), 269 (9%), 203 (adduct, 22%), 185 (adduct, 13%), 175 (100%), 157 (66%)	4.86 (<i>m</i>), 2.23 (<i>t</i> , 2H), 1.60–1.20 (<i>m</i>), 1.15 (<i>d</i> , 3H), 0.84 (<i>t</i> , 3H)	173.29, 70.71, 35.92, 34.59, 31.70, 29.06, 28.74, 25.33, 24.85, 22.52, 19.96 (CH ₃), 14.00
g	397 ([<i>M</i> + 1] ⁺ , 35%), 395 ([<i>M</i> – 1] ⁺ , 15%), 381 ([<i>M</i> – CH ₃] ⁺ , 4%), 325 (5%), 313 (adduct, 8%), 285 (53%), 283 (7%), 267 (16%), 201 (adduct, 20%), 183 (adduct, 10%), 173 (100%), 155 (63%)	4.86 (septuplet), 2.38 (<i>m</i>), 2.20 (<i>m</i>), 1.98 (<i>d</i>), 1.86 (<i>m</i>), 1.65–1.22 (<i>m</i>), 1.15 (2 <i>d</i>), 0.92 (<i>d</i>), 0.86–0.82 (2 <i>t</i>)	173.26, 70.67, 35.87, 34.54, 31.67, 29.02, 28.70, 25.30, 24.81, 22.49, 19.92, 13.97

^aEntry numbers correspond to Table 1.

specific peaks as the literature values on similar compounds (39 and references therein) appear to be contradictory. The other signals can be assigned to the monoacid or monoalcohol moieties in agreement with literature data (39,40).

Low-temperature flow properties. Cold-flow improvers for conventional diesel are typically copolymers containing several carboxylic functional groups (such as ethylene vinyl acetate, acrylate, or methacrylate) attached to a paraffin backbone similar in structure and melting point properties to those of the fuel component molecules (41,42). In diesel fuels, crystalline growth occurs when long-chain hydrocarbons continue to adsorb in structured layers on the solid surface. As addi-

tive molecules co-crystallize onto the surface, functional groups attached to their backbone hinder growth habit by interfering with the orderly formation of the layers. Obviously, nucleation must be initiated prior to activation of these copolymers; thus, these additives are more effective in reducing PP than CP of diesel fuels. These copolymers, called pour point depressants (PPD), are typically most efficient at concentrations at an additive level (ppm).

An earlier study (7) showed that copolymer PPD for conventional diesel were also effective in reducing PP of biodiesel as well as biodiesel/diesel blends. As was the case for conventional diesel fuel, copolymer PPD did not signifi-

cantly affect CP of biodiesel or blends. This indicates that mechanisms associated with crystalline growth habit are similar for biodiesel; that is, wax crystal growth and agglomeration in biodiesel occur by formation of structured layers.

As discussed previously, branched-chain esters such as isopropyl and 2-butyl esters of fats and oils typically have better low-temperature flow properties than their corresponding straight-chain isomers. Comparison of neat esters shows that bulky moieties in the short-chain alkyl group (headgroup) had reduced PP compared to esters with straight-chain headgroups. Thus, crystalline growth habit was hindered by the presence of the bulky headgroups. In contrast to treatment with copolymer PPD such as those discussed above, these esters themselves had reduced CP values, implying that the bulky moieties also interfere with formation of clusters of molecules that precede nucleation in bulk liquid solution. However, improvements in CP and PP were directly proportional to the blend level, meaning that a considerable volume of esters with branched-chain headgroups must be replaced with their branched-chain isomer to achieve significant improvement.

This study examines the hypothesis that compounds with bulky or branched-chain moieties at locations other than the headgroup (that is, within the midst of the structure) might be effective in hindering nucleation at additive level concentrations. Most of the compounds in Table 1 were structured with two straight-chain paraffinic or olefinic groups connected by ester linkages symmetrically about an aliphatic ring or branched-chain interior structure.

Methyl soyate gave CP = 0°C and PP = -3°C. Compounds synthesized in this study were evaluated at loadings of 2,000 ppm, a typically heavy concentration relative to treatment levels in the fuel industry. Compounds tested in this study had only minor effects (no more than 1°C), if any, on CP or PP parameters. Increasing loadings to 5,000 or 10,000 ppm yielded no significant benefits.

The relative ineffectiveness of these additives in decreasing PP suggests that the rates of additive co-crystallization were relatively low. As discussed previously, additives whose backbone structure has melting properties similar to those of crystallizing fuel molecules are most effective in reducing PP. With one exception, each of the additives in Table 1 had melting points 10°C or more below the PP of methyl soyate. Thus it is feasible that the physical properties of the basic molecular structure (perhaps in part due to the nature of the bulky moiety itself) of these additives precluded establishment of a significant rate of co-crystallization following initial formation of crystal nuclei by saturated fatty methyl ester molecules. The melting point of a straight-chain polymer is largely a function of chain length and its degree of unsaturation. Thus, future trials should consider lengthening the chains and/or reducing the number of double bonds in the tailgroup structure to facilitate compatible melting properties.

The only additive that did not have a low melting point was 1,4-cyclohexanedimethanol bis-laurate (MP = 53–56°C). Given that the melting point of methyl stearate is 37.8°C (43),

this compound likely initiated crystallization in the mixture at lower temperatures. Nevertheless, it is feasible that this additive had a significant rate of co-crystallization.

It is known that during crystallization of neat methyl stearate the molecules align themselves head-to-head in bilayers with carboxylic headgroups in proximity with each other (44). If, in a mixture with methyl soyate, the rate of co-crystallization of 1,4-di(hydroxymethyl)cyclohexane bis-laurate molecules was significant, it is likely these molecules aligned themselves in the crystal lattice with one or both ester linkages in proximity to the carboxyl groups of the saturated fatty methyl esters. Such an alignment may limit the effectiveness of the bulky aliphatic ring moiety with respect to altering the ordered alignment of tailgroups within the bilayers. Subsequent adsorption of saturated fatty methyl esters would occur with the ester tailgroups wrapping themselves about the bulky moiety with little or no alteration in the rate of crystal growth. These results indicate that future trials should examine modifying the nature and location of the bulky moiety for more effective hindering of crystalline growth habit.

ACKNOWLEDGMENTS

We thank Dale W. Ehmke, Haifa Khoury, Amanda L. Callison, and Rebecca (Burke) Zick for excellent technical assistance.

REFERENCES

1. Knothe, G., R.O. Dunn, and M.O. Bagby, Biodiesel: The Use of Vegetable Oils and Their Derivatives as Alternative Diesel Fuels, in *ACS Symp. Ser. 666 (Fuels and Chemicals from Biomass)*, American Chemical Society, Washington, DC, 1997, pp. 172–208.
2. Dunn, R.O., G. Knothe, and M.O. Bagby, Recent Advances in the Development of Alternative Diesel Fuel from Vegetable Oils and Animal Fats, *Recent Res. Devel. Oil Chem. 1*:31–56 (1997).
3. Lee, I., L.A. Johnson, and E.G. Hammond, Use of Branched-Chain Esters to Reduce the Crystallization Temperature of Biodiesel, *J. Am. Oil Chem. Soc. 72*:1155–1160 (1995).
4. Foglia, T.A., L.A. Nelson, R.O. Dunn, and W.N. Marmer, Low-Temperature Properties of Alkyl Esters of Tallow and Grease, *Ibid. 74*:951–955 (1997).
5. Wu, W.-H., T.A. Foglia, W.N. Marmer, R.O. Dunn, C.E. Goering, and T.E. Briggs, Low-Temperature Property and Engine Performance Evaluation of Ethyl and Isopropyl Esters of Tallow and Grease, *Ibid. 75*:1173–1178 (1998).
6. Lee, I., L.A. Johnson, and E.G. Hammond, Reducing the Crystallization Temperature of Biodiesel by Winterizing Methyl Soyate, *Ibid. 73*:631–636 (1996).
7. Dunn, R.O., M.W. Shockley, and M.O. Bagby, Improving the Low-Temperature Properties of Alternative Diesel Fuels: Vegetable Oil-Derived Methyl Esters, *Ibid. 73*:1719–1728 (1996).
8. Dunn, R.O., Effect of Winterization on Fuel Properties of Methyl Soyate, in *Proceedings of the Third Commercialization of Biodiesel Conference: Producing a Quality Biodiesel Fuel*, edited by C.L. Peterson, University of Idaho, Moscow, ID, 1998, pp. 164–186.
9. Dunn, R.O., M.W. Shockley, and M.O. Bagby, Winterized Methyl Esters from Soybean Oil: An Alternative Fuel with Improved Low-Temperature Flow Properties, *SAE Techn. Pap. Ser. 971682*, published in *State of Alternative Fuel Technologies SP-1274*, SAE, Warrendale, PA, 1997, pp. 133–142.
10. Fujii, K., M. Izumi, and M. Nakahara (Sanken Kako Co., Ltd.),

- Lubricating Oils for Refrigerators Using Tetrafluoroethane as Refrigerant, Japanese Patent 4,183,789 (1992).
11. Cornils, B., J. Weber, P. Lappe, H. Springer, E. Preisegger, and R. Henrici (Hoechst AG), The Use of Ester Oils as Lubricants in Refrigeration Compression, Eur. Pat. Appl. EP 445,611 (1991).
 12. Suzuki, N., J. Nishi, and Y. Ishii, Lubricants Containing Fatty Acid Esters for Processing Thermoplastic Synthetic Fibers, Japanese Patent JP 03 33,627 [91 33,267].
 13. Koch, K.H., and H. Kroke (Henkel und Cie. GmbH), Ester Lubricants and Hydraulic Fluids, German Patent 2,302,918 (1974).
 14. Goethel, H., and H. Feichtinger (Ruhchemie AG), Lubricants Based on Aliphatic Carboxylic Acid Diesters, German Patent 1,912,486 (1970).
 15. Aylesworth, R.D., and R.H. Boehringer (Emery Industries, Inc.), Blends of Ester Lubricants, U.S. Patent 3,309,318 (1967).
 16. Nanu, I., and R.F. Pape, Weichmachereigenschaften von Diestern mit Neoalkylstruktur, *Plaste Kautsch.* 26:301–306 (1979).
 17. Nanu, I., and R.F. Pape, Diesters of Neopentyl Glycol. Evaluation of Plasticizing Properties, *Mater. Plast. (Bucharest)* 16:218–220 (1979). *Chem. Abstr.* 92:164673x.
 18. Uehara, K., and H. Katsura (Shiseido Co., Ltd.), Cosmetic Neopentyl Glycol Esters, Japanese Patent 80 02,648 (1980).
 19. Finley, J.W., and A. Scimone (Nabisco, Inc.), Diol Lipid Analogs as Edible Fat Replacers, U.S. Patent 5,286,512 (1994).
 20. Givens, P.S., Jr., E.L. Wheeler, R.P. D'Amelia, M.S. Otterburn, G.A. Leveille, J.W. Finley, and L.P. Klemann (Nabisco Brands, Inc.), Cyclohexyl Diol Diesters as Low-Calorie Fat Mimetics, U.S. Patent 5,006,351 (1989).
 21. Isa, H., T. Inagaki, Y. Shimizu, and M. Nagayama (Lion Fat and Oil Co., Ltd.), Esters of Polyhydric Alcohols, Japanese Patent 75 62,925 (1975).
 22. Shinei Kagaku, K.K., and K.K. Shinko Kagaku, C₂₂-Dihydric Alcohol Mixture, Japanese Patent 80,167234 (1980).
 23. Bhatnagar, A.K., and K.K. Bhattacharyya, Synthetic Ester Lubricants: Pt. I—Synthesis and Properties of 2,2,-Dialkyl-1,3-propanediol Esters, *J. Indian Chem. Soc.* 58:594–596 (1981).
 24. Bochkova, V.A., V.A. Proskuryakov, K.V. Puzitskii, S.D. Pirozhkov, and Y.T. Eidus, Synthesis and Properties of Esters of α,α -Dimethylalkanoic Acids and Polyhydric Alcohols, *Zh. Prikl. Khim. (Leningrad)* 46:1818–1822 (1973). *Chem. Abstr.* 79:125776v.
 25. Volkova, I.A., V.A. Proskuryakov, and V.V. Gromova, Esters of Dodecanedioic Acid with Monohydric Alcohols, *Okislenie Uglevodorodov, Ikh Proizvod. Bitumov*: 15–19 (1971), from *Rfe. Zh., Khim.* 1972, Abstract No. 24Zh181. *Chem. Abstr.* 79:4962u.
 26. Ucciani, E., M. Schmitt-Rozieres, A. Debai, and L.C. Comeau, Enzymatic Synthesis of Some Wax Esters, *Fett/Lipid* 98: 206–210 (1996).
 27. Zeman, A., P. Bartl, and A. Schaaff, Die massenspektrometrische Fragmentierung von Neopentylpolyolestern. III. Neopentylglycolidfettsäureester, *Fette Seifen Anstrichm.* 80: 388–392 (1978).
 28. Zeman, A., P. Bartl, and A. Schaaff, Die massenspektrometrische Fragmentierung von Neopentylpolyolestern. I. Pentaerythrittetrafettsäureester, *Org. Mass Spectrom.* 13: 248–253 (1978).
 29. Zeman, A., P. Bartl, and A. Schaaff, Die massenspektrometrische Fragmentierung von Neopentylpolyolestern. II. Trimethylolpropanfettsäureester, *Fette Seifen Anstrichm.* 80: 278–282 (1978).
 30. Zeman, A., P. Bartl, and A. Schaaff, Die massenspektrometrische Fragmentierung von Neopentylpolyolestern. IV. Di- und Tripentaerythritfettsäureester, *Ibid.* 80:262–267 (1980).
 31. Zeman, A., P. Bartl, A. Schaaff, and V. Christ, Analyse synthetischer Flugturbinenöle durch Gas Chromatographie–Massenspektrometrie. Teil I. Pentaerythritesteröle, *Fresenius Z. Anal. Chem.* 290:21–28 (1978).
 32. Zeman, A., P. Bartl, and A. Schaaff, Analyse synthetischer Flugturbinenöle durch Gas Chromatographie–Massenspektrometrie. Teil II. Trimethylolpropan-Dipentaerythritesteröle, *Ibid.* 293: 4–10 (1978).
 33. Zeman, A., Analyse synthetischer Schmieröle auf Esterbasis durch Gas Chromatographie–CI(NH₃)–Massenspektrometrie, *Ibid.* 310:243–249 (1982).
 34. Kiiko, V.M., V.V. Gromova, and V.A. Proskuryakov, Study of the Composition of Products of the Thermal Decomposition of Neopentyl Glycol Ester by a Chromato-Mass Spectrometric Method, *Zh. Prikl. Khim. (Leningrad)* 53:2554–2556 (1980). *Chem. Abstr.* 94:174253r.
 35. LeTellier, P.R., and W.W. Nawar, Mass Spectrometry of Some Ethane- and Propanediol Diesters, *J. Agric. Food Chem.* 23:642–645 (1975).
 36. Baumann, W.J., J. Seufert, H.W. Hayes, and R.T. Holman, Mass Spectrometric Analysis of Long-Chain Esters of Diols, *J. Lipid Res.* 10:703–709 (1969).
 37. Knothe, G., and K.D. Carlson, Synthesis, Mass Spectrometry and Nuclear Magnetic Resonance Characterization of Di-Guerbet Esters, *J. Am. Oil Chem. Soc.* 75:1861–1866 (1998).
 38. Murphy, R.C., Fatty Acids, in *Mass Spectrometry of Lipids, Handbook of Lipid Research* 7, Plenum Press, New York, 1993, pp. 71–130.
 39. Breitmaier, E., and W. Voelter, *Carbon-13 NMR Spectroscopy*, 3rd edn., VCH, Weinheim, 1989.
 40. Gunstone, F.D., High Resolution ¹³C NMR Spectroscopy of Lipids, in *Advances in Lipid Methodology—Two*, edited by W.W. Christie, The Oily Press, Dundee, 1993, pp. 1–68.
 41. Chandler, J.E., F.G. Horneck, and G.I. Brown, The Effect of Cold Flow Additives on Low Temperature Operability of Diesel Fuels, in *SAE Tech. Paper Ser., Paper No. 922186*, Society of Automotive Engineers, Warrendale, PA, 1992.
 42. Lewtas, K., R.D. Tack, D.H.M. Beiney, and J.W. Mullin, Wax Crystallisation in Diesel Fuel: Habit Modification and the Growth of *n*-Alkane Crystals, in *Advances in Industrial Crystallisation*, edited by J. Garside, R.J. Davey, and A.G. Jones, Butterworth-Heinemann, Oxford, 1991, pp. 166–179.
 43. *The Lipid Handbook*, edited by F.D. Gunstone, J.L. Harwood, and F.B. Padley, Chapman and Hall, London, 1994, p. 1.
 44. *Ibid.*, p. 428.

[Received August 3, 1999; accepted May 31, 2000]